6th European Conference on Computational Mechanics (ECCM 6)
7th European Conference on Computational Fluid Dynamics (ECFD 7)
11 – 15 June 2018, Glasgow, UK

IMPACT OF GASOLINE SURROGATES WITH DIFFERENT FUEL SENSITIVITY (RON-MON) ON KNOCK PREDICTION

CORINNA NETZER[1,*], LARS SEIDEL[2], HARRY LEHTINIEMI[3], FRÉDÉRIC RAVET[4], FABIAN MAUSS[1]

[1] Thermodynamic and Thermal Process Engineering, Brandenburg University of Technology,
03044 Cottbus, Germany,
corinna.netzer@b-tu.de, fabian.mauss@tdtvt.de, www.b-tu.de

[2] LOGE Deutschland GmbH,
03046 Cottbus, Germany,
lars.seidel@logesoft.com, www. logesoft.com

[3] LOGE AB,
22370 Lund, Sweden,
harry.lehtiniemi@logesoft.com, www. logesoft.com

[4] Renault S.A.S,
91510 Lardy, France,
frederic.ravet@renault.com, www.group.renault.com

Key words: auto-ignition, engine knock, detailed chemistry, ETRF, detonation theory

Abstract The gasoline octane rating describes the auto-ignition tendency of commercial gasoline. In simulations, a surrogate are used to represent the commercial gasoline. In this work, different complex surrogates, a Primary Reference Fuel, a Toluene Reference Fuel and three Ethanol containing Toluene Reference Fuels, are analyzed regarding their knock prediction. The surrogates are composed such that the Research Octane Number is the same. The auto-ignition events ahead of the flame front are predicted using 3D CFD and a combustion model based on the ETRF mechanism by Seidel (2017). The strength of the auto-ignition is determined using the detonation diagram by Bradley and co-workers (2002). Applying the different surrogates, ignition kernels of different size and reactivity are predicted. The results indicate a dependency on the local temperature history and the low temperature chemistry of the fuel species. The comparison of constant volume reactor predictions and transient simulations shows that the analysis of ignition delay time and octane rating solely is not sufficient if the knock tendency in engine simulations needs to be characterized.

1 INTRODUCTION

Modern Spark Ignition (SI) engine development is dominated by the trade-off between maximizing the fuel efficiency and avoiding harmful engine knock. More and more frequently, computational fluid dynamics simulations are used to determine the best design of combustion chamber components to maximise the fuel efficiency and avoid any knock. Beside the engine

design and operating mode, the fuel quality has a major impact on engine knock [1-3]. The auto-ignition tendency of the fuel is mostly described by the Research Octane Number (RON) and the Motored Octane number (MON), and their combination is referred to as octane sensitivity S=RON-MON. The octane rating was introduced more than 80 years ago and is still the only widely used gasoline rating. In simulations often Primary Reference Fuels (PRF) are applied to predict engine knock. Their composition of *iso*-octane (RON =100, MON =100) and *n*-heptane (RON = 0, MON = 0) can be used to compose a surrogate that represents the RON of a commercial gasoline fuel, but never at the same time the correct MON or octane sensitivity. Therefore, in recent years the use of surrogates for Toluene Reference Fuels (TRF) and ethanol containing Toluene Reference Fuels (ETRF) were proposed [4-6]. Thanks to a third or fourth fuel species, surrogates with close agreement in RON and octane sensitivity to real gasoline can be formulated [7]. A reaction scheme for ETRF surrogates allows modelling the impact of chemical and physical fuel properties on auto-ignition and knock behaviour in in-cylinder models. The benefit of detailed online chemistry models is the capability to capture the impact of exhaust gas recirculation (EGR) and radicals or NOx in the residual as discussed for example in [8, 9], and references therein. Further precise modelling of species formation (NOx, soot, radicals and unburned hydrocarbons) is possible, which is a requirement to capture cycle-to-cycle variation. The drawback of such reaction mechanisms is the higher number of species and therefore higher computational costs.

In this work, we analyse the effect of different surrogates on the engine knock prediction. Surrogates composed of different fuels (PRF, TRF, ETRF) are compared to each other. The applied surrogates have all the same RON, but differ in MON and other characteristics as C:H:O–ratio and density. Through this analysis, the effect of the different gasoline surrogates characteristics on engine knock prediction is evaluated. The aim is to understand the impact of the surrogate composition on the predicted knock intensity, the knock onset timing and the knock limit spark advance (KLSA).

2 METHODOLOGY

For this work, the knock prediction and evaluation methodology introduced in [10] is adopted and here shortly summarized: The combustion is modelled based on an ETRF reaction scheme from Seidel [11]. The core model is described in [12] and the reduction strategy in [13]. For this purpose, a combination of G-equation [14] and a well-stirred reactor model in the unburned zone to predict auto-ignition is applied. Both models are available in CONVERGE 2.4. [15]. The laminar flame speed for flame propagation is retrieved from look-up tables generated with LOGEsoft [16]. In contrast to the approach in [10], the same flame speed table for different surrogates is applied to reduce the number of influencing factors.

The analysis is carried out using a turbocharged spark ignition Renault passenger car engine with port-injection. The spark is initialized 4°CA before top dead centre, which was found in the experiments to be the KLSA using a commercial gasoline with RON 94.5/MON 84.1 (more details in Table 2). Operated at 2000 rpm, an indicated mean effective pressure of 10.6 bar is achieved. The engine geometry is given in Table 1. The port-injection is not modelled; ports and the cylinder are initialized homogenously. The base mesh size is set to 0.75 mm. Using the automatic mesh refinement (AMR) strategy [15] based on temperature and flow velocity, the mesh is refined at the flame front and chemical reactive regions down to 0.125 mm.

Table 1: Engine specification.

Bore, mm	72.0
Stroke, mm	82.0
Connecting rod, mm	128.0
Compression ratio, -	10.9

A post-processing strategy is used to evaluate the character and the severity of the auto-ignition event based on the detonation diagram by Bradley and co-workers [17-20]. Typically used knock indexes are calculated from the pressure fluctuations [21]. In contrast, the use of the detonation theory enables to analyse the auto-ignition in the unburned mixture, which is the origin of those pressure fluctuations. By the use of the regime classification, a distinction between auto-ignition events in deflagration and transition to harmful developing detonation, which corresponds in engines to knocking combustion, is possible. In the detonation diagram, resonance parameter ξ and the reactivity parameter ε characterized the combustion mode:

$$\xi = \frac{a}{u} = a\frac{\partial T}{\partial x}\frac{\partial \tau}{\partial T} \tag{1}$$

$$\varepsilon = \frac{l}{a\,\tau_e} \tag{2}$$

The resonance parameter is given by the ratio of the burning velocity u to the speed of sound a. If they are in the same order of magnitude, the two waves may combine and form a developing detonation. The reactivity parameter includes the initial radius of the ignition kernel l and is a measure for the hot spot reactivity. The resonance and the reactivity parameter have a direct dependency on fuel characteristics in terms of the ignition delay time τ and the excitation time τ_e. The borders of the developing detonation peninsula and engine relevant regimes are given

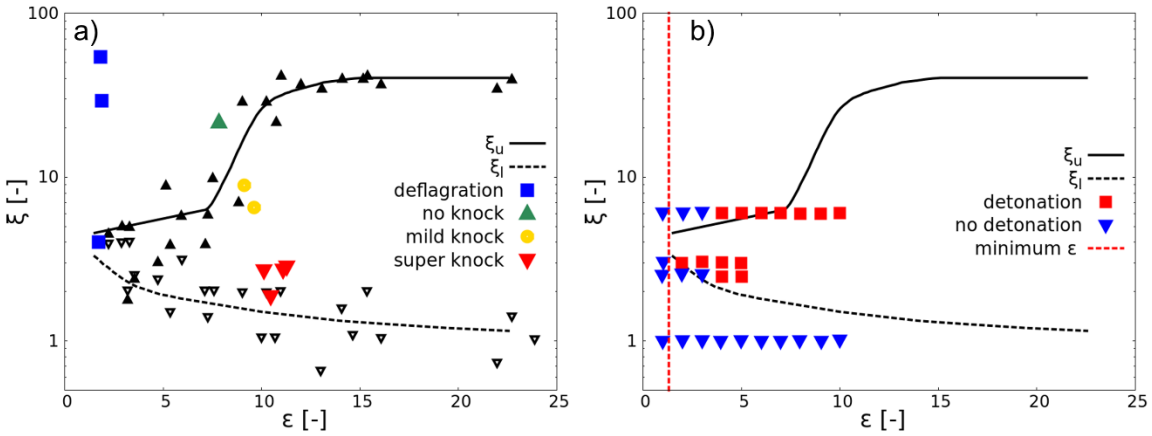

Figure 1: a) Triangles and lines: upper and lower bound of the developing detonation peninsula by Bradley et al. [17]. Remaining symbols are taken from Bates et al. [22]. b) Detonation boundaries verification and minimum ε for a developing detonation by Peters et al. [23].

in Figure 1. Peters et al [23] verified the developing detonation boundaries for *n*-heptane and *iso*-octane-air mixtures to be close to the original ones derived for a H_2-CO-air mixture and confirmed the minimum ε to 1.6. Further, it was stated that the high temperature chemistry is

the reason for the apparent fuel independence of the transition boundaries, since the high temperature chemistry is similar for the analysed fuels [23].

In the 3d CFD post-processing the ignition kernel size is measured and the thermodynamic properties such as hot spot temperature elevation is extracted. Ignition delay times τ and excitation times τ_e are calculated using constant volume reactors [16]. The post-processing strategy is introduced and in detail discussed in [10].

3 SURROGATES

Different surrogates with same RON, but different number of surrogate fuel species and therefore different MON are composed using the methodology discussed in [11], where correlations from Morgan et al. [6] and Anderson et al. [24] are applied. The developed correlation from Morgan et al. [6] is used to formulate the TRF surrogate for the gasoline fraction. The mixing rules for oxygenated fuels with gasoline suggested by Anderson et al. [24] are applied to determine the impact of the ethanol fraction. To compose the surrogates the aromatic content is represented by toluene. The ethanol fraction and the desired RON are input parameters. The *iso*-octane and *n*-heptane fractions of the surrogate are calculated to reproduce the desired RON. The physical and chemical properties of the composed surrogates are given in Table 2 and are illustrated in Figure 2 and Figure 3.

Table 2: Properties of the commercial gasoline (fuel analysis) and the surrogates (calculated).

	RON	**MON**	**S**	**aromatic content**	**ethanol content**	**ρ**	**LHV**	**M**	**C:H:O –ratio**
	-	**-**	**-**	**vol%**	**vol%**	**kg/m³**	**MJ /kg**	**g/mol**	**mass%**
Gasoline	94.5	84.1	10.4	32.6	0.0	747.5	42.9	-	86.9.13.1:0.0
PRF	94.5	94.5	0.0	0.0	0.0	691.3	44.4	113.4	84.2:15.8:0.0
TRF	94.5	88.2	6.3	32.6	0.0	747.3	42.9	103.1	86.9:13.1:0.0
ETRF 1	94.5	88.1	6.4	22.5	5.1	735.3	42.4	98.4	84.3:13.8:1.9
ETRF 2	94.6	87.6	7.0	18.8	10.9	728.5	41.7	93.3	82.0:14.2:3.8
ETRF 3	94.4	84.3	10.1	44.6	10.4	769.6	40.9	89.0	84.0:12.4:3.6

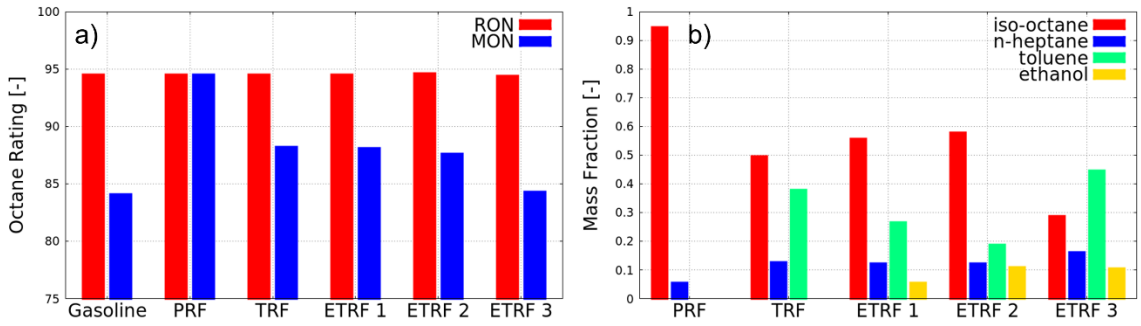

Figure 2: a) RON and MON of the commercial gasoline and the analysed surrogates. b) Composition of the analysed surrogates in mass fraction.

4 RESULTS AND DISCUSSION

The equivalence ratio ϕ is connected to fuel mass and air mass by definition:

$$\phi = \frac{m_{fuel}/m_{oxydizer}}{\left(m_{fuel}/m_{oxydizer}\right)_{stoichometric}} \tag{3}$$

In the simulation setup, it was chosen to set the air and fuel mass in the intake port for all surrogates to the same amount. Since all surrogates have different C:H:O-ratios and consequently a different stoichiometric air demand, the mass based equivalence ration ϕ differs about $\phi=1\pm 0.05$. There are also small deviations in trapped energy due to differences in lower heating value (LHV) and density ρ. The alternative to set $\phi=1$ for all surrogates, would lead to different trapped masses and different flow prediction during the load change. Correcting the fuel masses to compensate for different LHV in order to achieve the same trapped energy, would lead to small deviations from stoichiometric mixture and trapped masses also affecting the flow filed. The differences in ignition delay time τ prediction using constant volume reactors of the different surrogates and equivalence ratios are shown in Figure 3. A different trend of the PRF versus the TRF and ETRF surrogates is visible. Whereas for $\phi=1$ (dashed lines), the ignition delay time of the TRF and ETRF surrogates converge at 870 K and invert the trends at this temperature, this crossing temperature for the actual trapped mixtures with different equivalence ratios (solid lines) appears at about 820 K. For those predictions, the difference in ignition delay time are more pronounced at 900 K. The predicted ignition delay times are converted from milliseconds to crank angle degree for 2000 rpm (Figure 3 b)). At temperature >900 K the differences in ignition delay are about 1 °CA and higher. This would suggest a distinctive deviation in KLSA in the engine simulations due to the surrogate formulation if only considering ignition delay times. .

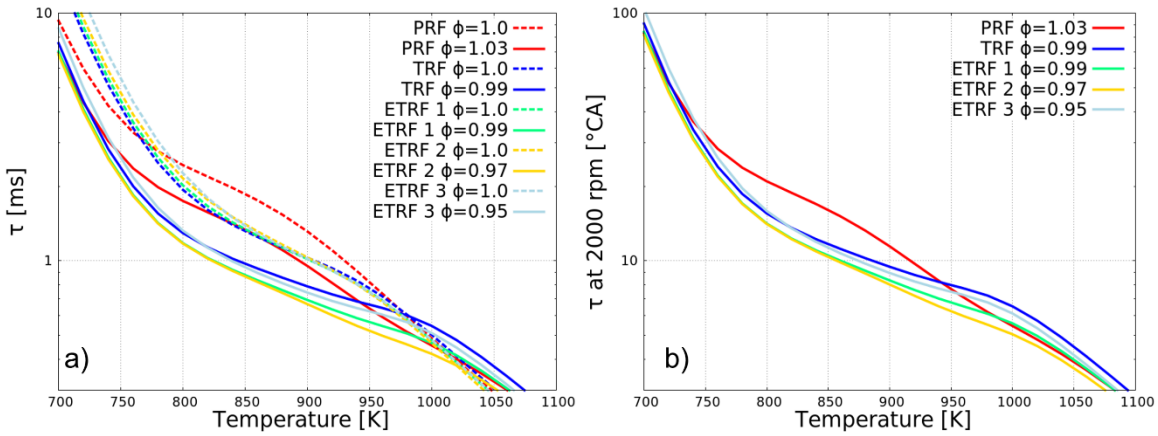

Figure 3: a) Predicted ignition delay time for different mixtures with air as oxidizer at 60 bar using constant volume reactors. b) Ignition delay time converted from milliseconds to crank angle degree for a speed of 2000 rpm.

The predicted mean pressure from 3d CFD for the different surrogates at the reference (ref) spark timing (ST) from the experiment are shown in Figure 4. Since the same flame speed table is used for all calculations the flame propagation prediction is close, the thermodynamic conditions in the unburned zone are comparable. For all surrogates a spark sweep from -2 °CA

to +1°CA related to the reference spark timing is performed. Exemplary, the predicted maximum pressure in the cylinder is shown for the spark sweep using ETRF 2 as surrogate. At about top dead centre (TDC) the spark modelled via an energy source is visible. Shortly before the maximum pressure is reached, fluctuations resulting from auto-ignitions in the unburned zone appear. The onset of those fluctuations delays and the amplitude decreases with delayed spark timing as it is expected from literature.

The predicted auto-ignitions in the unburned zone for all performed spark timings are evaluated using the detonation diagram (Figure 5 a)). Only for surrogate TRF and ETRF 2 the KLSA is found to be at the experimental reference spark timing. ETRF 2 shows the strongest auto-ignition events in the developing detonation regime, whereas for surrogate TRF the ignition kernels for ST -2°CA and -1°CA are very close to the transition line and therefore examined as developing detonation regime. Surrogate TRF agrees very well to the commercial gasoline properties used in the experiments. Figure 6 provides more information on the auto-ignition onset, the ignition kernel size, the maximum temperature in the ignition kernel prior the high temperature ignition and the mean pressure in the combustion chamber at the ignition.

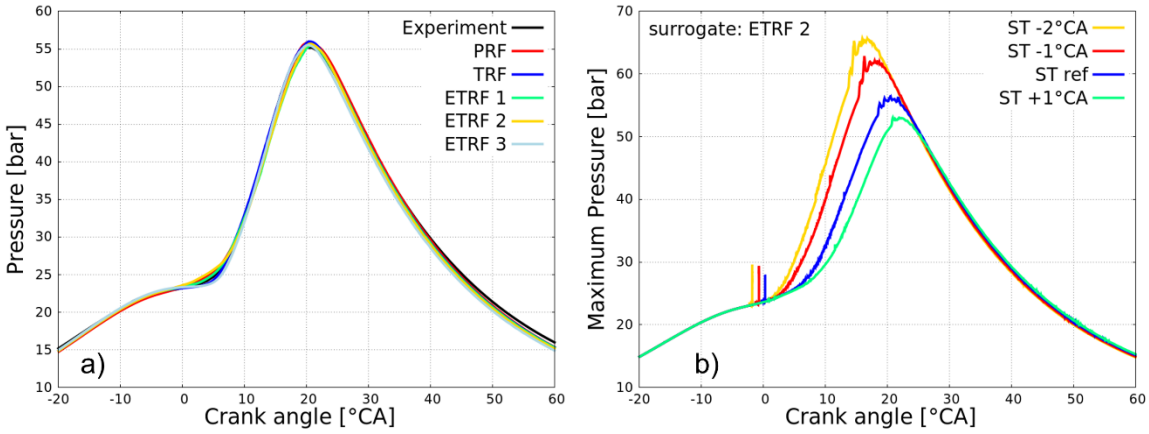

Figure 4: a) Predicted mean pressure for the analysed surrogates. b) Maximum predicted pressure for the spark timing sweep using surrogate ETRF 2.

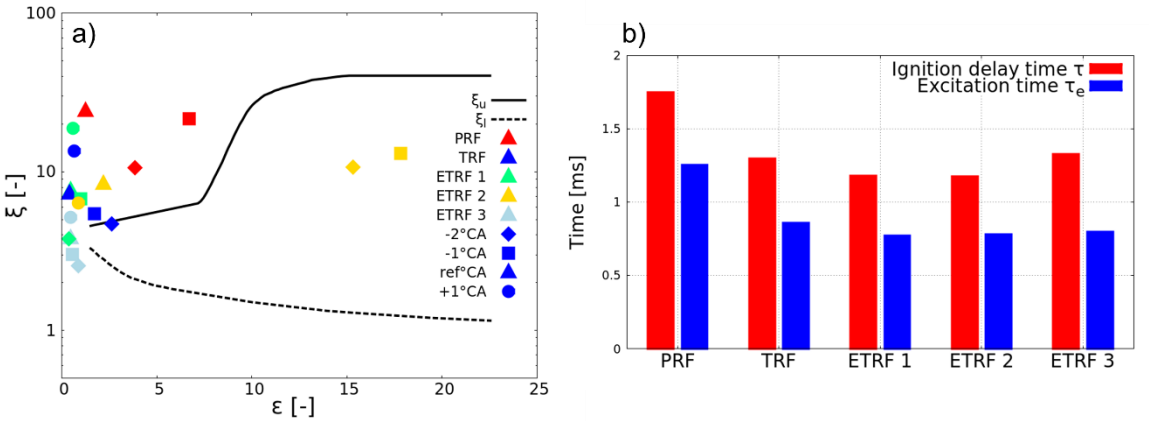

Figure 5: a) Evaluation of the auto-ignitions for the different surrogates and the spark timing sweep. If more than one auto-ignition is predicted, only the strongest is shown. b) Ignition delay and excitation times at 800 K and 60 bar.

The weakest auto-ignition kernels are predicted for the PRF surrogate (Figure 5). The auto-ignition onset is the latest, the temperatures prior the high temperature ignition the lowest and the ignition kernel sizes rather small. The combination of those effects leads to lower burning velocities during the ignition process. Even though the mean pressure of the calculation PRF ST -2°CA is predicted to be the highest (Figure 6 d)) the auto-ignition event is not potentially developing into a detonation (red square). This auto-ignition tendency follows from the ignition delay times shown in Figure 3 and the MON rating.

Surrogate TRF and ETRF 1 differ in their composition, but have the same MON and equivalence ratio in the engine simulation. However, the evaluation using the detonation diagram shows noticeable differences in the strengths of the auto-ignitions. Although there are larger ignition kernels formed using surrogate ETRF 1, the strength is evaluated to be weaker. The burning velocity u is higher than for surrogate TRF, which leads to smaller values in the resonance parameter, the transition line to developing detonation is not crossed. This goes together with lower maximum temperatures in the ignition kernel and lower mean pressures. Overall, a smaller reactivity for the kernels of surrogate ETRF1 and lower resulting gas velocities as result of the auto-ignition are predicted (Figure 7). Comparing the three ETRF surrogates, ETRF 2 forms the strongest auto-ignitions kernels and ETRF 3 the weakest. This finding agrees with the trend in ignition delay time τ, but disagrees in terms of MON. ETRF 3 has the lowest, ETRF 1 the highest MON. Considering only this characteristic number the trends in auto-ignition tendency are unexpected. Several reasons might contribute to this finding: The suggested MON values for toluene differ in literature from MON = 104.0 [25] to MON = 109.0 [26]. To calculated the MON in this work MON = 109.0 is applied as it is reported by Heywood [2] and following the rules from Morgan et al [6]. Further the difference in MON = 88.1 (ETRF 1) and MON = 87.6 (ETRF 2) are within the reproducibility and repeatability

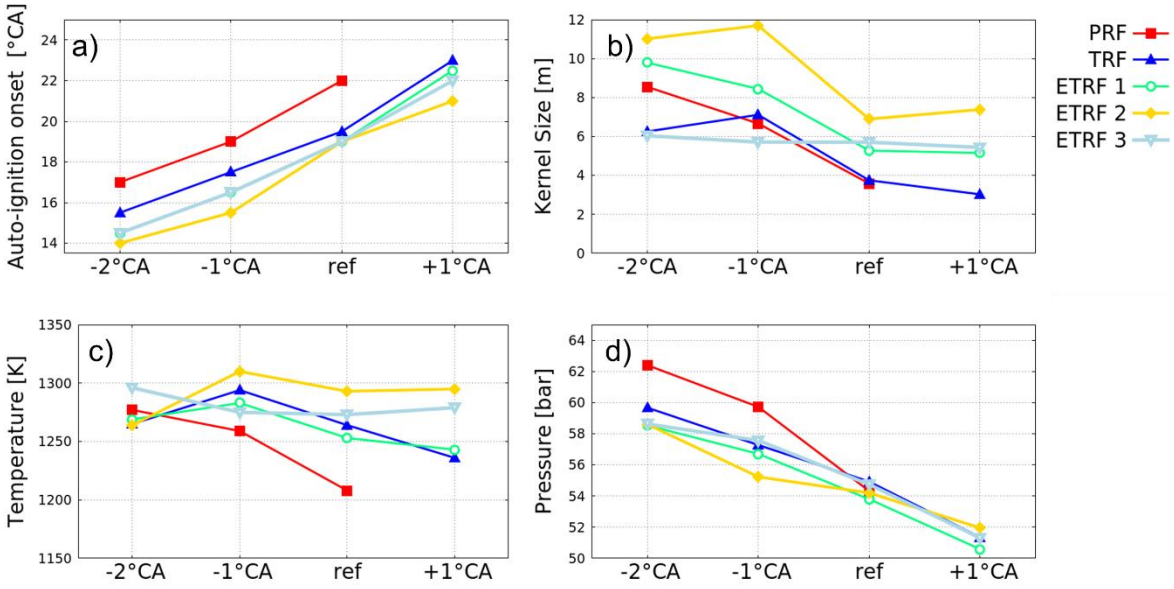

Figure 6: Selected properties of the predicted ignition kernels. a) Onset of auto-ignition b) Kernel size prior ignition (extracted based on mass fraction CH_2O) c) Maximum temperature in the ignition kernel prior ignition d) Mean pressure in the domain at the auto-ignition event.

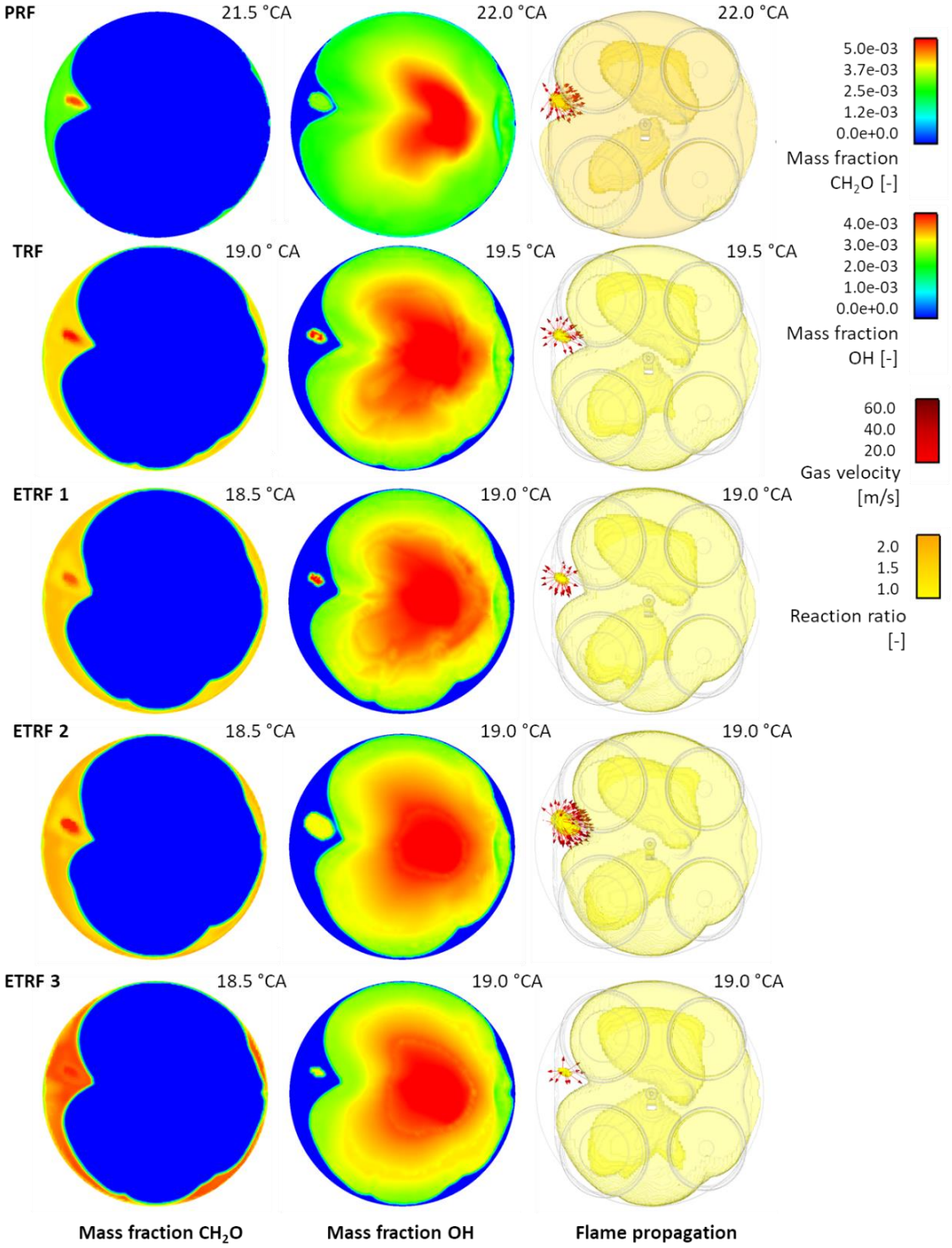

Figure 7: Time step of first auto-ignition event and previous. From left to right: Mass fraction CH_2O, mass fraction OH and flame propagation determined from an iso-volume at reaction ratio ≥ 1.0 and gas velocity. View from top.

limits discussed in [3, 25, 26]. Further, this engine operating point with a boost pressure of 1.5 bar and 2000 rpm differs to the MON test conditions. The predicted ignition delay times >820 K show a different trend in auto-ignition tendency than the MON numbers suggest (Figure 3 and 5 b)). Further, ETRF 2 leads to the biggest ignition kernels and highest maximum temperatures in those ignition kernels even though they are very similar in RON and MON. Moreover, effects from differences in equivalence ratios, in heat capacity and local flow field may superpose the effect of MON. This becomes clearer when studying the kernel development of ETRF 3.

In Figure 7 the low temperature chemistry is illustrated on the example of formaldehyde CH_2O. The level of CH_2O in the unburned zone in the time step prior auto-ignition is the lowest for the PRF and increases with increasing *n*-heptane, which has pronounced low temperature chemistry, amount up to ETRF 3. In those figures, it can also be seen that the ignition kernels appear in the same region for all calculations at reference spark timing since the flame propagation and flow field are similar. The reactivity of the ignition kernels is illustrated using the OH radical as high temperature marker and the gas velocity vectors. Both agree, with the evaluation of the auto-ignition in the detonation diagram. ETRF 2 has clearly the strongest auto-ignition event, surrogate PRF has an ignition kernel size that is similar to the ones of TRF, ETRF 1 and ETRF 2, but is less reactive. Even though ETRF 3 shows the highest concentration of the low temperature marker CH_2O, it shows the lowest concentration of OH and the smallest reacted burned volume (Figure 7, bottom row centre). It is very likely that there is less energy available in the ignition kernel due to the smaller ϕ and lower LHV. At this crank angle, the energy released by auto-ignition competes against the quenching by expansion and it may be possible that the kernel cannot release sufficient energy to develop a detonation. To understand if this lower knock tendency can be explained with homogenous reactors the species profiles are analysed.

Figure 8 shows tow typical low temperature chemistry species CH_2O, an early *iso*-octane decomposition product C_8H_{17} and the average temperature. The species mass and temperature profiles are shown for different reactor models:

- Constant volume reactors that are typically used to calculated ignition delay times.
- Results from a homogenous rapid compression machine (RCM) model imposing the engine volume profile and inlet conditions to consider the same transient effects as in the CFD engine simulation.
- Results from the 3d CFD simulation.

In the constant reactor simulation, low temperature chemistry occurs the earliest for the PRF, which is not the case in the transient RCM and CFD simulation. The CH_2O concertation is lower as for the other surrogates as it is also predicted in the transient simulations. ETRF 2 has the earliest CH_2O formation in the transient calculations and leads to the strongest knock events in the CFD simulation. ETRF 1 has a lower tendency to auto-ignite than ETRF 2 in the RCM and CFD simulation, but not in the constant volume reactor calculations. From the RCM calculation, it can be seen that ETRF 3 reaches a higher compression pressure and temperature, but releases the least energy in the expansion. The TRF mixture has longer ignition delay times in the constant volume reactor calculations, but is on the second rank in knock tendency in the engine simulation. This points out, that solely form homogenous calculations (constant volume or RCM) no conclusion on the knock tendency can be drawn.

The same study was performed using the ETRF mechanism from Cai et al [27]. Even though the scheme ignites much earlier, we found the same trends for the ETRF surrogates, but no clear connection between the homogenous calculations and the knock tendency in the CFD calculation.

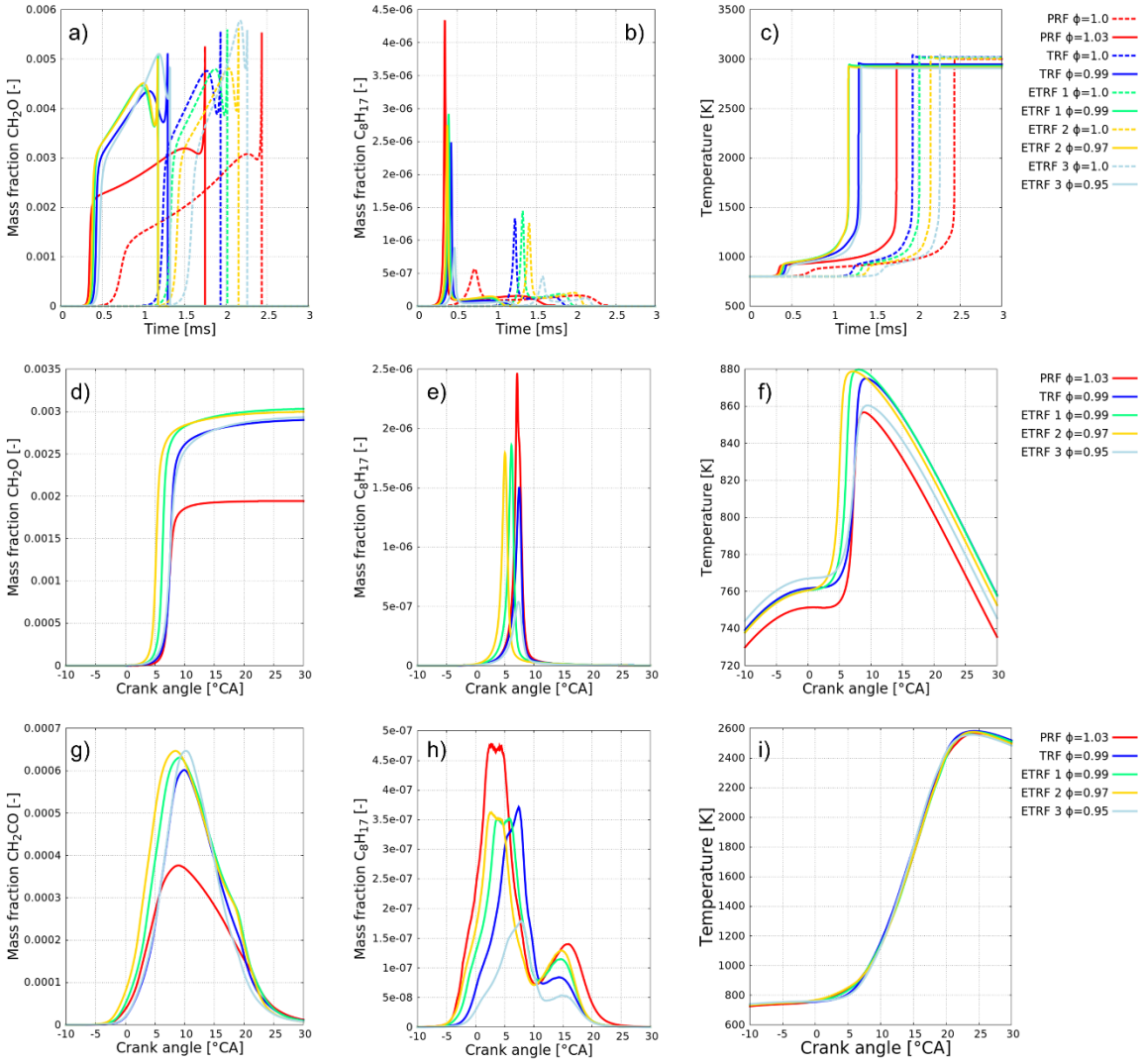

Figure 8: Predicted mass fractions of typical low temperature chemistry species and temperature profiles for different simulation types: a) – c) constant volume reactor with inlet 800 K and 60 bar d) –e) rapid compression machine g) - i) CFD.

5 CONCLUSIONS

Surrogates with same RON, but different MON have been composed using *iso*-octane, *n*-heptane, toluene and ethanol as fuel surrogate species. The composed PRF, TRF and ETRF surrogates have been analysed regarding their auto-ignition and knock tendency using constant volume reactors, rapid compression machine and 3d CFD engine simulations. To make the study comparable, the same flow field in the CFD simulation was achieved by keeping air mass and fuel mass constant. This leads to ignition kernel appearance at the same position.

Even though the surrogates have the same RON, the tendency to auto-ignite in the engine simulations is very different. The found shift in KLSA is 2 °CA and bigger. No clear connections between MON and knock tendency or ignition delay time in homogenous reactors and knock tendency was found. The predicted sensitivities may also depend on the specific surrogate properties such as density, heat capacity, lower heating value and C:H:O-ratio.

The KLSA predicted using TRF surrogate, which corresponds the best to the commercial gasoline, is found to be the same as in the experiment.

We found that it is not possible to estimate the knock tendency of different surrogates in the CFD simulation from homogenous reactor calculations. This finding is irrespective of the used reaction scheme, but may be influenced by the physical properties of the analysed surrogates.

REFERENCES

[1] Ricardo, H. R., Schnellaufende Verbrennungsmaschinen, Springer-Verlag Berlin Heidelberg GmbH, 1926.

[2] Heywood, J.B, Internal Combustion Engine Fundamentals, New York: McGraw Hill, 1988.

[3] Merker, G.P. ,Schwarz, C., Teichmann, R., Combustion Engines Development, Springer-Verlag Berlin Heidelberg, 2012.

[4] Gauthier, B. M., Davidson, D. F., & Hanson, R. K., "Shock tube determination of ignition delay times in full-blend and surrogate fuel mixtures," *Combust Flame,* vol. 139(4), p. 300–311, 2004.

[5] Andrae, J.C.G., Björnholm, P., Cracknell, R.F., Kalghatgi, G.T., "Autoignition of touluene refererence fuels at high pressures modeled with detailed chemical kinetics," *Combust Flame,* vol. 149, pp. 2-24, 2007.

[6] Morgan, N., Smallbone, A., Bhave, A., Kraft, M., Cracknell, R., Kalghatgi, G., "Mapping surrogate gasoline compositions into RON/MON space," *Combust Flame,* vol. 157(6), p. 1122–1131, 2010.

[7] Pera, C. and Knop, V., "Methodology to define gasoline surrogates dedicated to auto-ignition in Engines," *Fuel,* vol. 96, pp. 59-69, 2012.

[8] Stenlåås, O., Gogan, A., Egnell, R., Sundén, B., Mauss, F., "The Influence of NO on the Occurrence of Autoignition in the End Gas of SI-Engines," *SAE Technical Paper 2002-01-2699,* 2002.

[9] Hoffmeyer, H., Montefrancesco, E., Beck, L., Willand, J., Ziebert, F., Mauss, F., "CARE – Catalytic Reformated Exhaust gases in turbocharged DISI-Engines," *SAE Technical Paper 2009-01-0503,* 2009.

[10] Netzer, C., Seidel, L., Pasternak, M., Lehtiniemi, H., Perlman, C., Ravet, F., Mauss, F., "Three-dimensional computational fluid dynamics engine knock prediction and evaluation based on detailed chemistry and detonation theory," *Int J Engine Res,* vol. 19 (1), pp. 33-44, 2018.

[11] Seidel, L., Development and Reduction of a Multicomponent Reference Fuel for Gasoline, Brandenburg University of Technology Cottbus-Senftenberg: PhD thesis, 2017.

[12] Seidel, L., Moshammer, K., Wang, X., Zeuch, T., Kohse-Höinghaus, K., Mauss, F., "Comprehensive kinetic modeling and experimental study of a fuel-rich, premixed n-heptane flame," *Combust Flame,* vol. 162(5), p. 2045–2058, 2015.

[13] Seidel, L., Netzer, C., Hilbig, M., Mauss, F., Klauer, C., Pasternak, M., Matrisciano, A., "Systematic Reduction of Detailed Chemical Reaction Mechanisms for Engine Applications," *J Eng Gas Turb Power,* Vols. 139 - 091701, 2017.

[14] Peters, N., Turbulent Combustion, Cambridge University Press, 2000.

[15] Richards, K. J., Senecal, P. K., and Pomraning, E.,, "CONVERGE (v2.4), Convergent Science, Inc., Madison, WI," 2017.

[16] *LOGEsoft v1.08,* LOGE AB, www.logesoft.com, 2016.

[17] Bradley, D., Morley, C., Gu X. J., Emerson D. R., "Amplified Pressure Waves During Autoignition: Relevance to CAI Engines," *SAE Technical Paper 2002-01 -2868,* 2002.

[18] Gu, X.J., Emerson, D.R.; Bradley, D., "Modes of reaction front propagation from hot spots," *Combust Flame,* vol. 133, p. 63–74, 2003.

[19] Bradley, D., and Kalghatgi, G.T., "Influence of autoignition delay time characteristics of different fuels on pressure waves and knock in reciprocating engines," *Combust Flame,* vol. 156, pp. 2307-2318, 2009.

[20] Kalghatgi, G.T., and Bradley, D., "Pre-ignition and ‘super-knock’ in turbocharged spark-ignition engines," *SAE Int J Engines,* vol. 13(4), pp. 399-414, 2015.

[21] Zhen, X., Wang, Y., Xu, S., Zhu, Y., Tao, C., Xu, T., Song, M., "The engine knock analysis – An overview," *Appl Energ,* vol. 92, p. 628–636, 2012.

[22] Bates, L., Bradley, D., Paczko, G., Peters, N., "Engine hotpots: Modes of auto-ignition and reaction propagation," *Combust Flame,* vol. 166, pp. 80-85, 2016.

[23] Peters, N., Kerschgens, B., Jochim, B., Paczko, G., "Mega knock in super-charged gasoline engines interpreted as a localized developing detonation," *4th International Conference on Knocking in Gasoline Engines, Berlin,* 2013.

[24] Anderson, J., Leone, T., Shelby, M., Wallington, T. et al., "Octane Numbers of Ethanol-Gasoline Blends: Measurements and Novel Estimation Method from Molar Composition," *SAE Technical Paper 2012-01 -1274,* 2012.

[25] Spausta, F., Eigenschaften und Untersuchungen der flüssigen Treibstoffe: die gasförmigen Treibstoffe, Springer-Verlag Wien, 2nd edition, 1953.

[26] Knop, V., Loos, M., Pera, C., and Jeuland, N., "A linear-by-mole blending rule for octane and numbers of n-heptane/iso-octane/toluene mixtures," *Fuel,* vol. 120, pp. 240-242, 2014.

[27] Cai, L. and Pitsch, H., "Optimized chemical mechanism for combustion of gasolines surrogate fuels," *Combust Flame,* vol. 162(5), pp. 1623-1637, 2015.